

UvA-DARE (Digital Academic Repository)

Dynamics of high-*n* Rydberg states employed in zero kinetic energy-pulsed field ionization spectroscopy via the F 1D₂, D 1P₁, and f 3D₂ Rydberg states of HCl.

Wales, N.P.L.; Buma, W.J.; de Lange, C.A.; Lefebvre-Brion, H.

DOI

[10.1063/1.472415](https://doi.org/10.1063/1.472415)

Publication date

1996

Published in

Journal of Chemical Physics

[Link to publication](#)

Citation for published version (APA):

Wales, N. P. L., Buma, W. J., de Lange, C. A., & Lefebvre-Brion, H. (1996). Dynamics of high-*n* Rydberg states employed in zero kinetic energy-pulsed field ionization spectroscopy via the F 1D₂, D 1P₁, and f 3D₂ Rydberg states of HCl. *Journal of Chemical Physics*, *105*, 5702-5710. <https://doi.org/10.1063/1.472415>

General rights

It is not permitted to download or to forward/distribute the text or part of it without the consent of the author(s) and/or copyright holder(s), other than for strictly personal, individual use, unless the work is under an open content license (like Creative Commons).

Disclaimer/Complaints regulations

If you believe that digital publication of certain material infringes any of your rights or (privacy) interests, please let the Library know, stating your reasons. In case of a legitimate complaint, the Library will make the material inaccessible and/or remove it from the website. Please Ask the Library: <https://uba.uva.nl/en/contact>, or a letter to: Library of the University of Amsterdam, Secretariat, Singel 425, 1012 WP Amsterdam, The Netherlands. You will be contacted as soon as possible.

Dynamics of high- n Rydberg states employed in zero kinetic energy-pulsed field ionization spectroscopy via the $F^1\Delta_2$, $D^1\Pi_1$, and $f^3\Delta_2$ Rydberg states of HCl

N. P. L. Wales, W. J. Buma, and C. A. de Lange

Laboratory for Physical Chemistry, University of Amsterdam, Nieuwe Achtergracht 127,
1018 WS Amsterdam, The Netherlands

H. Lefebvre-Brion

Laboratoire de Photophysique Moléculaire, Bâtiment 213, Université de Paris-Sud, 91405 Orsay Cedex,
France

(Received 24 May 1996; accepted 5 July 1996)

The intensity anomalies in the spin-orbit and rotational branching ratios in the zero kinetic energy pulsed-field ionization (ZEKE-PFI) spectra via the $F^1\Delta_2$, $D^1\Pi_1$, and $f^3\Delta_2$ Rydberg states of HCl have been studied. In general, the branching ratios are observed to depend on three parameters employed in the pulsed field ionization experiment: (i) the delay time between excitation and ionization; (ii) the magnitude of the bias electric field; and (iii) the magnitude of the applied pulsed electric field. The results can be rationalized on the basis of the increasing number of autoionization decay channels that become available to the high- n Rydberg states as each ionization threshold is surpassed. The delay dependence of the ZEKE-PFI spectra via the $F^1\Delta_2$ state has been analyzed in more detail by *ab initio* calculations. These calculations show that the observed spin-orbit branching ratios can be reproduced thereby giving evidence for a nonexponential decay of the high- n Rydberg states ($n \approx 100$). © 1996 American Institute of Physics. [S0021-9606(96)02638-4]

I. INTRODUCTION

Zero kinetic energy-pulsed field ionization (ZEKE-PFI) has been shown to be a powerful tool for studying the ionization dynamics and deriving accurate spectroscopic parameters of small molecules.¹ In the past this information has been obtained, by and large, using one-photon or resonance enhanced multiphoton ionization photoelectron spectroscopy (REMPI-PES) techniques. These methods are, however, hindered by their lack of resolution (≈ 10 meV) and more often than not do not allow for rotationally resolved photoelectron spectra to be obtained. In this aspect ZEKE-PFI offers tremendous advantages due to its superior resolution which is in principle laser bandwidth limited.

In the absence of perturbing factors such as energy-dependent photoionization matrix elements, the ionic branching ratios in both kinds of spectra are expected to be more or less the same. In contrast, for those cases where photoelectron spectra can be obtained with rotational resolution it has been shown that it is more the rule, rather than the exception that large differences are observed with the corresponding ZEKE-PFI spectra. Two proposals have been advanced to explain these differences. The first explanation is based on "forced" autoionization upon application of the pulsed extraction field due to the interaction between high- n Rydberg states, assumed to be responsible for the ZEKE-PFI intensity, and low- n Rydberg states converging upon higher ionic thresholds.² This mechanism can be considered as a purely gaining mechanism. The second mechanism, in contrast, focuses on differences in lifetimes of high- n Rydberg states converging upon different ionic thresholds as a result of rotational and spin-orbit autoionization.^{3,4} With pulsed field ionization the losses due to different decay rates then are

directly reflected in the ionic branching ratios.

The former explanation has been invoked and investigated in various studies. However, as yet no *ab initio* calculations incorporating this mechanism have been performed to analyze its effects quantitatively. The second mechanism, on the other hand, is more amenable to experimental and theoretical investigations, and is indeed the subject of the present study, in which ZEKE-PFI spectroscopy has been performed on HCl after two-photon excitation of parity-selected rotational levels of the $F^1\Delta_2$, $D^1\Pi_1$, and $f^3\Delta_2$ Rydberg states. These states are in a one-configuration picture described mainly by $[^2\Pi_{1/2}]4p\pi$, $[^2\Pi_{1/2}]4p\sigma$, and $[^2\Pi_{3/2}]4p\pi$, respectively. On the basis of these configurations the $F^1\Delta_2$ and $D^1\Pi_1$ states are expected to ionize predominantly to the $^2\Pi_{1/2}$ ionic state, as has been confirmed by previous REMPI-PES studies, which showed spin-orbit branching ratios $^2\Pi_{3/2}:^2\Pi_{1/2}$ of approximately 1:6^{5,6} and 1:16⁷ for ionization via the $F^1\Delta_2$ and $D^1\Pi_1$ states, respectively. Similarly, the $f^3\Delta_2$ state is predicted to ionize predominantly to the $^2\Pi_{3/2}$ ionic state. Here a $^2\Pi_{3/2}:^2\Pi_{1/2}$ ratio of 6:1⁶ has been observed.

In our experiments we study the dependence of the spin-orbit and rotational branching ratios in the ZEKE-PFI spectra of the three above mentioned Rydberg states on the time delay between excitation and field ionization of the high- n Rydberg states, the magnitude of the bias electric field employed to sweep out promptly generated photoelectrons, and the magnitude of the pulsed electric field. In the case of the $F^1\Delta_2$ state, excitation of the $J'=2$ intermediate level is performed via the $S(0)$ and $P(3)$ transitions, thereby allowing for the investigation of the influence of alignment in the intermediate state. Similarly, the $P(2)$ and $P(3)$ tran-

sitions to the $D^1\Pi_1$ state are used to study the effects of varying J' . Finally, the $S(0)$ transition is used in the experiments *via* the $f^3\Delta_2$ state.

A qualitative inspection of the obtained ZEKE-PFI spectra gives direct evidence for the dominant role of rotational and spin-orbit autoionization mechanisms, since spin-orbit and rotational branching ratios are observed to depend critically on the time delay, bias, and pulsed electric field. A more precise, quantitative analysis will be performed for the ZEKE-PFI spectra *via* the $F^1\Delta_2$ state by a comparison of experimental with simulated spectra obtained by *ab initio* calculations, which take the autoionization decay into account. It will be shown that the results of the experiments can be explained, if a nonexponential decay behavior is assumed for the population of the high- n Rydberg states involved in the ZEKE-PFI process, in agreement with previous experimental⁸ and theoretical results for similar cases.^{9,10}

II. EXPERIMENT

The main experimental apparatus has been discussed in detail before,¹¹ and only aspects concerning the ZEKE-PFI setup will be discussed. Briefly, in the ionization chamber of a ‘‘magnetic bottle’’ time-of-flight spectrometer two grids have been installed on the magnetic pole faces for the purpose of applying static and/or pulsed electric fields. In the present ZEKE-PFI experiments the grid nearest the flight tube is grounded, while at the other grid a negative variable bias is applied (-0.5 to -2.5 V, corresponding to an electric field strength of 2.5 to 12.5 V/cm). After a certain time delay an electric field is switched on which can be varied up to -5.0 V, corresponding to an electric field strength of 25 V/cm. For the majority of the ZEKE-PFI experiments delays of the pulsed electric field of 5 ± 5 and 105 ± 5 ns have been employed, although in case of the $F^1\Delta_2$ state a time delay of 30 ± 5 ns has been used as well. The uncertainty in the time delay of approximately 10 ns originates from the full width half maximum of the laser pulse. In our experiments a time delay longer than about 100 ns was not practical for two reasons. First, the tight focusing used in the experiments and the spatial restrictions on the homogeneity of the magnetic field, which dramatically influence the electron collection efficiency, limit the drifting time of high- n Rydberg states. Secondly, in order to be absolutely sure that effects due to high charge densities, such as collision-induced ionization, would be absent, the powers of excitation and probe lasers have been attenuated to such an extent that only very weak PFI signals could be obtained. Absence of saturation was confirmed by the proportionality of the ZEKE-PFI signal to the probe laser intensity. At all time delays various combinations of bias and pulsed electric field strengths were used.

The laser system consists of two dye lasers (Lumonics HD300 and HD500) simultaneously pumped by a XeCl excimer laser (Lumonics HyperEX 460). The output of the first dye laser (HD500), operating on Coumarin 480, was frequency doubled (HyperTrak 1000) using a BBO crystal, generating tunable UV radiation between 234 and 250 nm. The UV light was subsequently focused by a quartz lens (focal

length 25 mm) into the ionization chamber and used to pump various rovibronic levels of the $F^1\Delta_2$, $D^1\Pi_1$, and $f^3\Delta_2$ Rydberg states of HCl situated at the two-photon level. The fundamental output of the second dye laser (HD300), also operating on Coumarin 480, was focused by an identical lens on the opposite side of the spectrometer and scanned over the $^2\Pi_{3/2}$ and $^2\Pi_{1/2}$ rotational ionic thresholds. Both dye lasers were overlapped in time using a fast silicon photodiode (HP5082), and intersected an effusive beam of pure HCl (99.8% HoekLoos) at right angles.

Since in this study the main emphasis of our interpretation is based upon the observed rotational and spin-orbit branching ratios, correction for the dye gain curve is essential. This was done by simultaneously measuring the probe laser intensity during the experiments with a fast silicon photodiode (HP5082) and dividing the observed ZEKE-PFI signal by the measured intensity.

III. RESULTS AND DISCUSSION

A. Experimental observations

Figures 1 and 2 depict ZEKE-PFI spectra obtained *via* the $P(3)$ and $S(0)$ rotational transitions of the $F^1\Delta_2$ ($v'=0$) Rydberg state, respectively. These spectra are the result of employing various combinations of bias and pulsed electric fields at two delay times. The spectra clearly demonstrate that the observed intensities of the ionic rotational levels in the ZEKE-PFI spectra are affected by the time delay of the pulsed electric field, the magnitude of the bias electric field, and the size of the pulsed electric field.

The following qualitative observations on the rotational and spin-orbit branching ratios can be made for ZEKE-PFI ionizing *via* the $F^1\Delta_2$ Rydberg state. The delay time influences the branching ratios two-fold in going from 5 to 105 ns. First, the spin-orbit branching ratio $^2\Pi_{1/2}:^2\Pi_{3/2}$, taken as the ratio summed over rotational lines $I(^2\Pi_{1/2}):I(^2\Pi_{3/2})$ and denoted in the following as I_R , decreases for a longer delay time while keeping other parameters constant. Secondly, the rotational distribution over the $^2\Pi_{3/2}$ ionic manifold is affected. Intensity is transferred from the $J^+\geq 5/2$ levels to the $J^+=3/2$ level, which consequently dominates the spectra for the long time delay. Within experimental error, however, no changes are observed in the $^2\Pi_{1/2}$ rotational branching ratios. In the spectra I_R is observed to become smaller upon increasing the bias electric field from 2.5 to 10 V/cm. Varying the bias electric field also affects the rotational branching ratios to the $^2\Pi_{3/2}$ ionic state in a similar way as has been observed for the delay time, i.e., intensity is transferred to the $J^+=3/2$ level. However, once again no changes are observed within the $^2\Pi_{1/2}$ rotational manifold. When the spectra are examined more closely, we observe that when the bias electric field is increased the $J^+=5/2(^2\Pi_{3/2})$ ZEKE-PFI peak decreases faster in intensity than ionic rotational levels with $J^+\geq 7/2(^2\Pi_{3/2})$. Finally, increasing the electric field pulse broadens the ZEKE-PFI lines, as expected, but in addition I_R decreases with minor changes occurring in the rotational branching ratio to the $^2\Pi_{3/2}$ and $^2\Pi_{1/2}$ ionic states. Although the ZEKE-PFI spectra obtained after excitation *via* $S(0)$ and

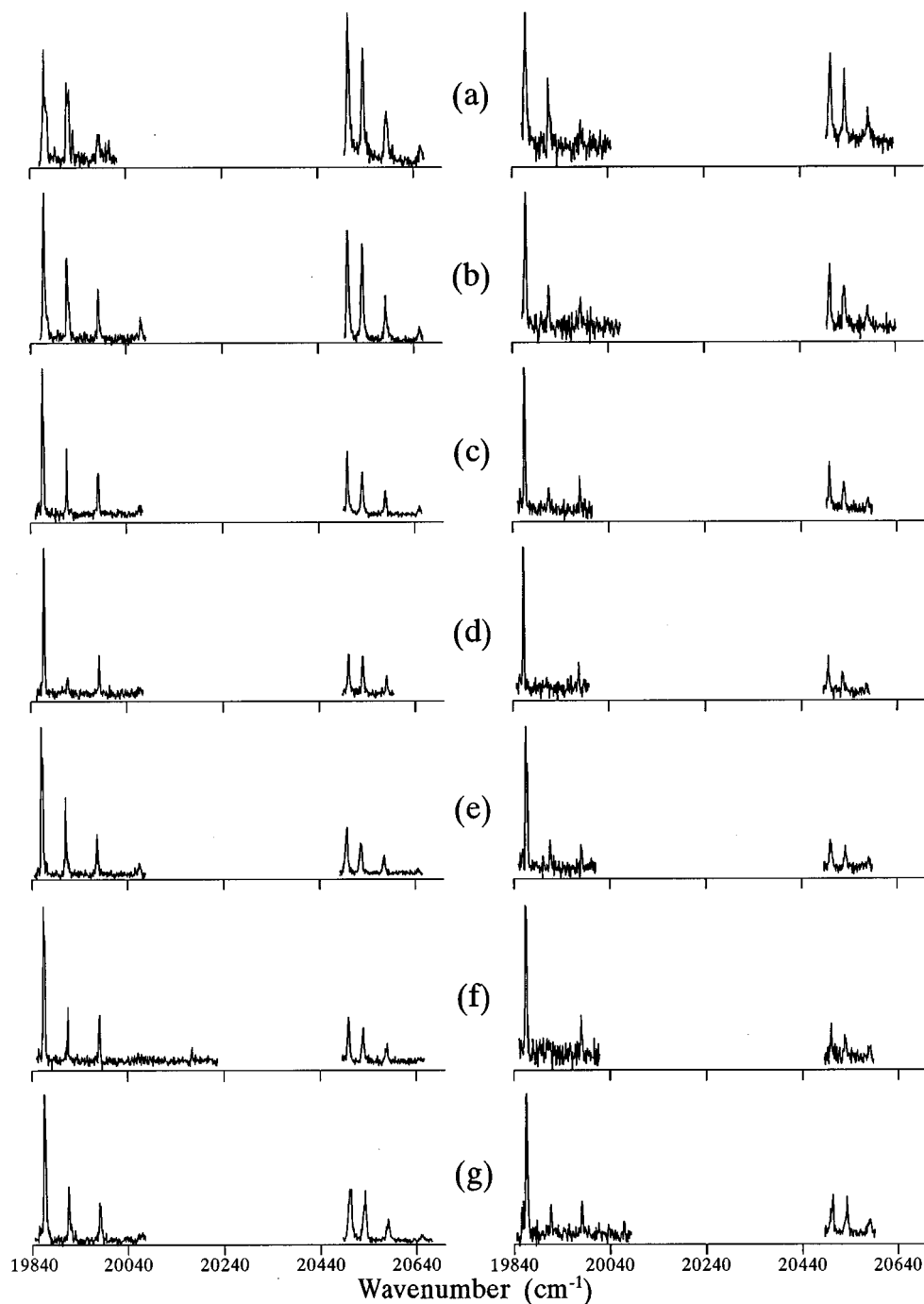


FIG. 1. ZEKE-PFI spectra *via* the $P(3)$ rotational transition to the $F\ ^1\Delta_2(v'=0)$ Rydberg state. The spectra in the left hand column were obtained for a time delay of 5 ± 5 ns, the spectra in the right hand column for a time delay of 105 ± 5 ns. The following combinations of bias field and bias+pulse fields (V/cm) were used: (a) (2.5, 7.5); (b) (5.0, 10.0); (c) (7.5, 12.5); (d) (10.0, 15.0); (e) (5.0, 12.5); (f) (7.5, 15.0); (g) (5.0, 15.0).

$P(3)$ seem to depend qualitatively in the same way on the three parameters investigated here, a quantitative comparison shows that they exhibit different behaviors.

Shown in Figs. 3 and 4 are ZEKE-PFI spectra resulting from ionization *via* the $P(2)$ and $P(3)$ rotational transitions associated with the $D\ ^1\Pi_1(v'=0)$ Rydberg state, respectively. The observations made for the $F\ ^1\Delta_2$ ZEKE-PFI spectra above also hold for ionizing *via* this state. In addition, the spin-orbit and rotational branching ratios change dramati-

cally in going from $J'=1$ to $J'=2$. The intensity in the $J^+=3/2(^2\Pi_{3/2})$ ZEKE-PFI peak is dominant in all the spectra *via* the $P(3)$ rotational transition. As a result the changes in the spin-orbit and rotational branching ratios are not as clear as for the $P(2)$ rotational transition.

The pulse, bias electric field, and time delay dependencies for ionization *via* the $f\ ^3\Delta_2(v'=0)$ Rydberg state have also been investigated. Ionization takes place almost solely to the $^2\Pi_{3/2}$ ionic state. The spectra depicted in Fig. 5 show

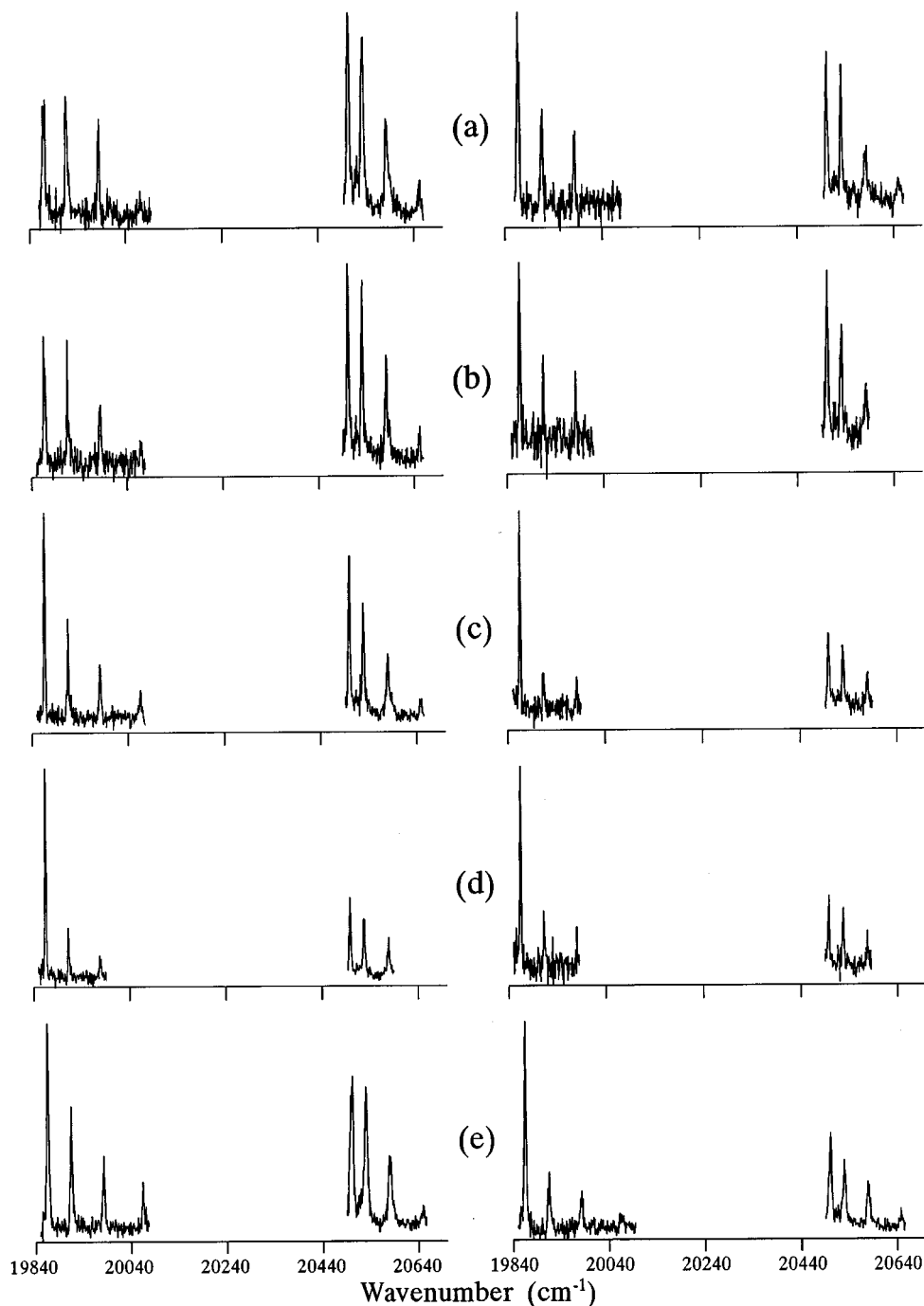


FIG. 2. ZEKE-PFI spectra *via* the $S(0)$ rotational transition to the $F^1\Delta_2$ ($v'=0$) Rydberg state. The spectra in the left hand column were obtained for a time delay of 5 ± 5 ns, the spectra in the right hand column for a time delay of 105 ± 5 ns. The following combinations of bias field and bias+pulse fields (V/cm) were used: (a) (2.5, 7.5); (b) (5.0, 10.0); (c) (7.5, 12.5); (d) (10.0, 15.0); (e) (5.0, 15.0).

no significant changes in the $^2\Pi_{3/2}$ rotational branching ratios when the various parameters are changed. However, it is important to note that the ratio $I(^2\Pi_{3/2}):I(^2\Pi_{1/2})$ is larger than that obtained when employing the REMPI-PES technique⁶ as has been shown in Ref. 4. Because of the extremely weak ZEKE-PFI signals at the $^2\Pi_{1/2}$ rotational ionic thresholds, it was difficult to monitor the effects of changing the various parameters on the spin-orbit branching ratio. The fact that the latter ratio is larger when using ZEKE-PFI in-

dicates, however, that spin-orbit autoionization reduces the available high- n Rydberg states converging upon the $^2\Pi_{1/2}$ rotational limits for extraction by pulsed field ionization.

B. Theoretical calculations

Simulations of the ZEKE-PFI spectra *via* the $F^1\Delta_2$ state were performed following the method described in Ref. 4. It is important to note that these calculations take rotational as

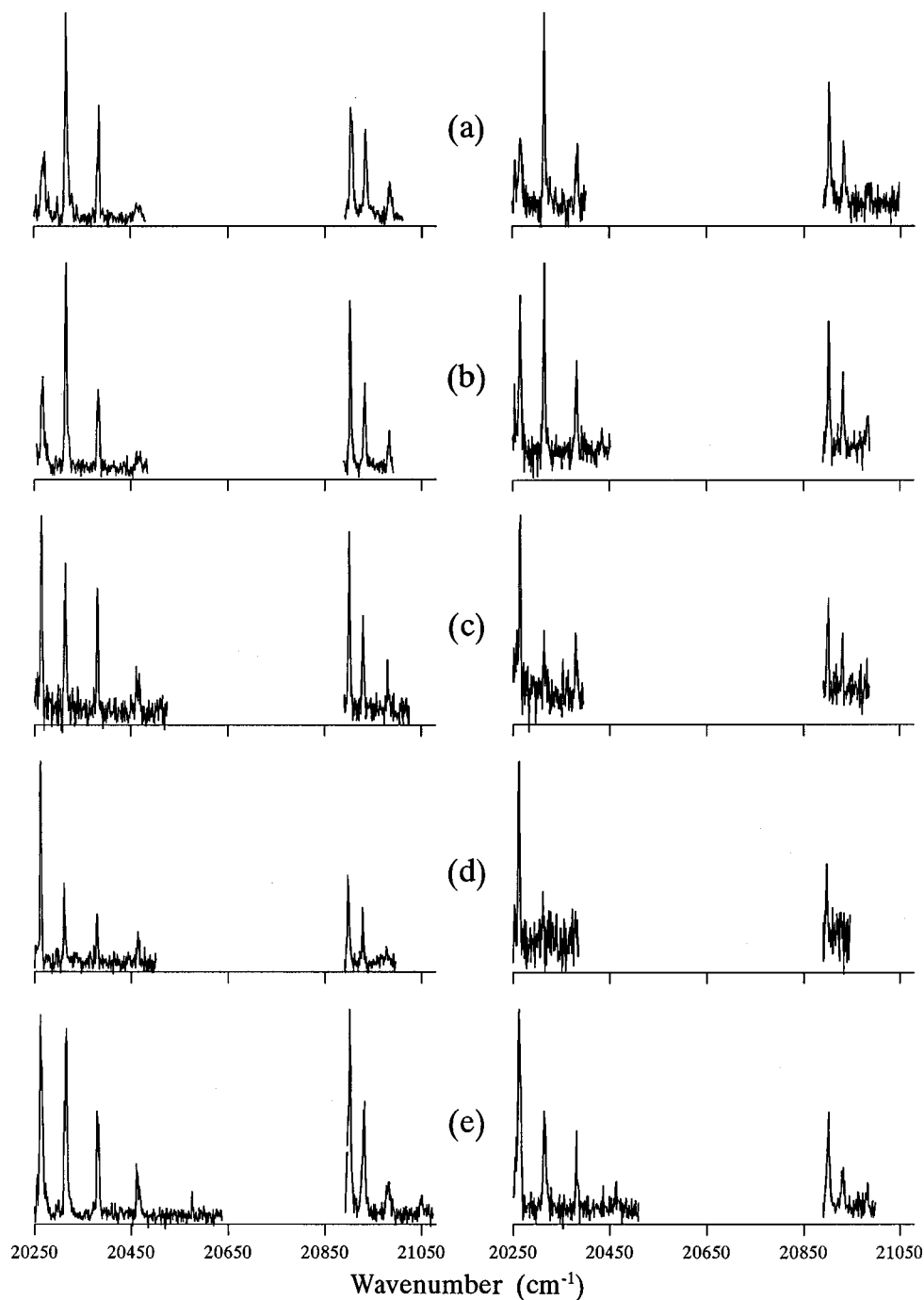


FIG. 3. ZEKE-PFI spectra via the $P(2)$ rotational transition to the $D\ ^1\Pi_1$ ($v'=0$) Rydberg state. The spectra in the left hand column were obtained for a time delay of 5 ± 5 ns, the spectra in the right hand column for a time delay of 105 ± 5 ns. The following combinations of bias field and bias+pulse fields (V/cm) were used: (a) (2.5, 7.5); (b) (5.0, 10.0); (c) (7.5, 12.5); (d) (10.0, 15.0); (e) (5.0, 15.0).

well as spin-orbit autoionization into account, thereby allowing for a direct analysis of the decay dynamics of the high- n Rydberg states during the delay time. For a time delay of 0 ns ZEKE-PFI spectra were obtained identical to those reported in Ref. 12 without alignment taken into account, except that in the present calculations the singlet-triplet mixing in the $F\ ^1\Delta_2$ state was explicitly included. This means that, similarly to the REMPI-PES spectra, the $X\ ^2\Pi_{1/2}$ ionic state is dominant with a ratio I_R of 6.5.⁵

During the time delay the high- n Rydberg states converging upon the various rotational ionic thresholds of the $X\ ^2\Pi_{3/2}$ state decay by rotational autoionization, except those converging upon the $J^+=3/2$ level for which no open channels are available. As a result the intensities of the $J^+>3/2$ ZEKE-PFI lines are diminished. Similarly, the intensities of the $^2\Pi_{1/2}$ rotational lines are affected by both rotational and spin-orbit autoionization, but more than the $^2\Pi_{3/2}$ lines since the number of open channels is increasing with energy.

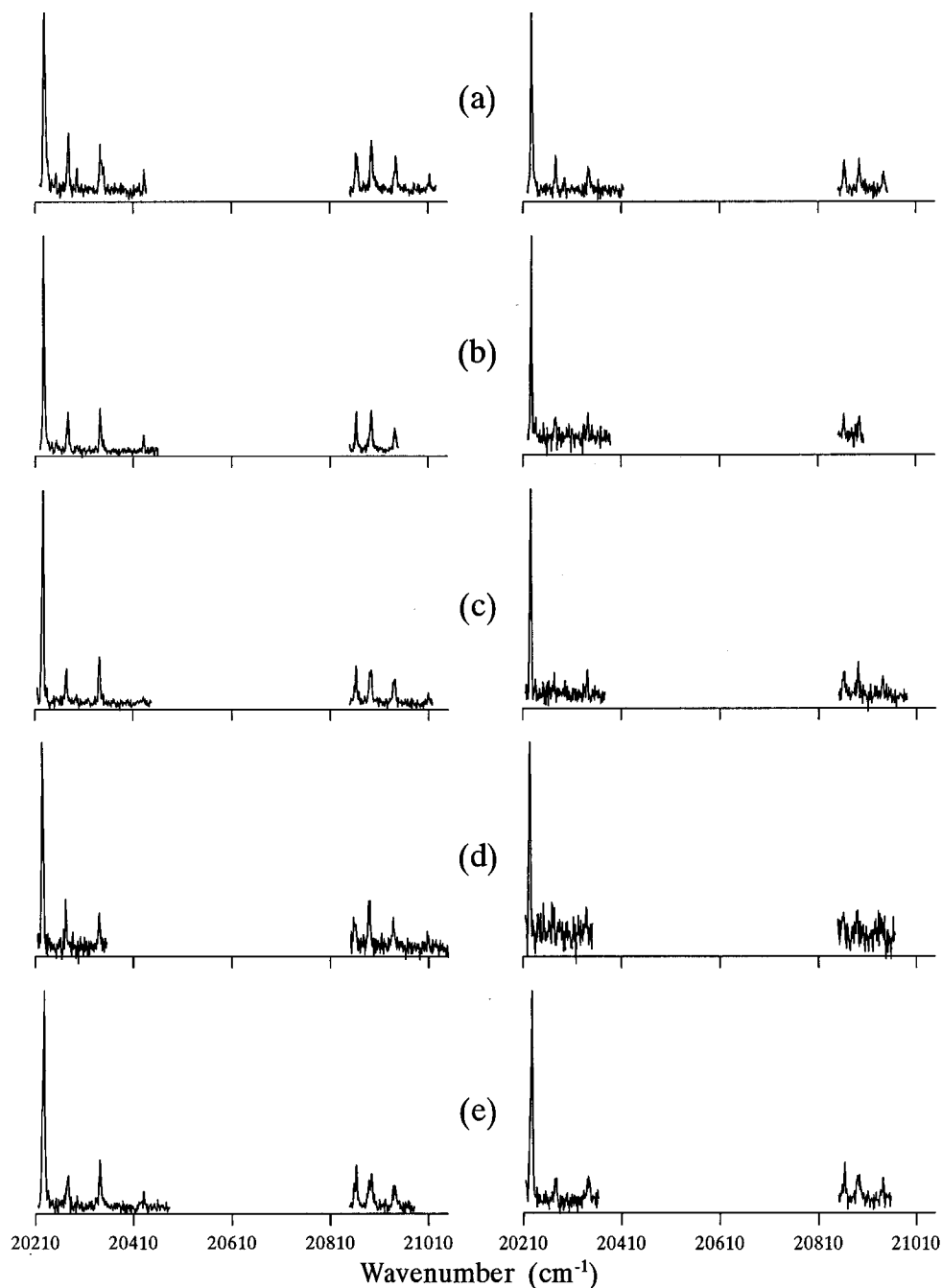


FIG. 4. ZEKE-PFI spectra *via* the $P(3)$ rotational transition to the $D^1\Pi_1$ ($v'=0$) Rydberg state. The spectra in the left hand column were obtained for a time delay of 5 ± 5 ns, the spectra in the right hand column for a time delay of 105 ± 5 ns. The following combinations of bias field and bias+pulse fields (V/cm) were used: (a) (2.5, 7.5); (b) (5.0, 10.0); (c) (7.5, 12.5); (d) (10.0, 15.0); (e) (5.0, 15.0).

Hence, I_R decreases in agreement with experimental observations. Although qualitative agreement is readily found, quantitative agreement between the measured and calculated I_R values can only be obtained if the calculation is not performed for a value of n_{field} which is calculated from the Stark shift due to the employed bias and pulsed fields, but for a value multiplied by a scaling factor S . Effectively, this amounts to increasing the lifetimes of the high- n Rydberg states, which are proportional to $(n \cdot S)^3$, by a “dilution factor” $D(n) = S^3$ [see Fig. 6(a)].

If the same scaling factor is retained for the simulation of the spectrum after a delay of 30 ns, the simulation predicts that all the peaks would disappear in the ZEKE-PFI spectrum, except for the first peak associated with the $J^+ = 3/2$ level of the $X^2\Pi_{3/2}$ ionic manifold. In other words, under the conditions assumed for the dilution factor the decay due to rotational and spin-orbit autoionization is so fast that hardly any of the Rydberg states converging upon higher rotational and spin-orbit ionic thresholds survive the time delay. In order to obtain agreement with experiment, it is necessary to

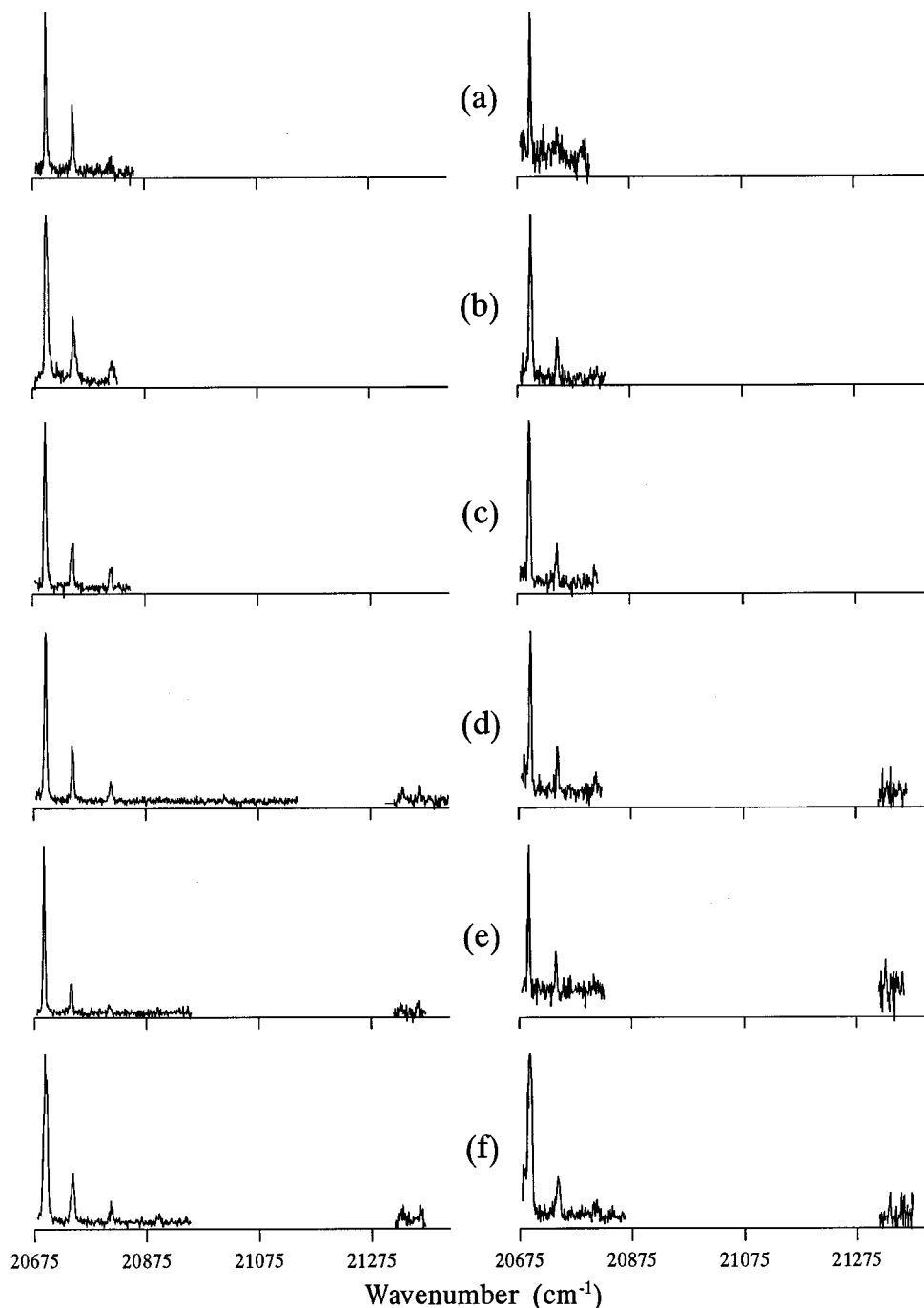


FIG. 5. ZEKE-PFI spectra via the $S(0)$ rotational transition to the $f^3\Delta_2$ ($v'=0$) Rydberg state. The spectra in the left hand column were obtained for a time delay of 5 ± 5 ns, the spectra in the right hand column for a time delay of 105 ± 5 ns. The following combinations of bias field and bias+pulse fields (V/cm) were used: (a) (2.5, 5.0); (b) (1.0, 6.0); (c) (2.5, 7.5); (d) (5.0, 10.0); (e) (10.0, 15.0); (f) (5.0, 15.0).

increase the scaling factor [see Fig. 6(b)]. The same conclusion is reached when the spectrum obtained after a delay of 105 ns is considered with the dilution factor appropriate for the 30 ns time delay: once again $D(n)$ needs to be increased to achieve agreement between experiment and theory [see Fig. 6(c)].

It is important to note that the *same* dilution factor should have been found for *all* values of the time delay, if the decay of the high- n Rydberg states would have been monoexponential. In contrast, the present analysis shows that

this is not the case, with lifetimes in the order of 5–25 ns for the short time delay range, which become about ten times longer after 100 ns (see Table I). Exact quantitative conclusions are more difficult to give, due to the experimental uncertainty in the time delay and the signal-to-noise ratios obtained in the spectra. It should be realized that the uncertainty of 10 ns in the time delay and the lifetimes of 5–25 ns in the range of short time delays leads one to expect significant variations in the experimental values of I_R from one experiment to another performed under the “same” ex-

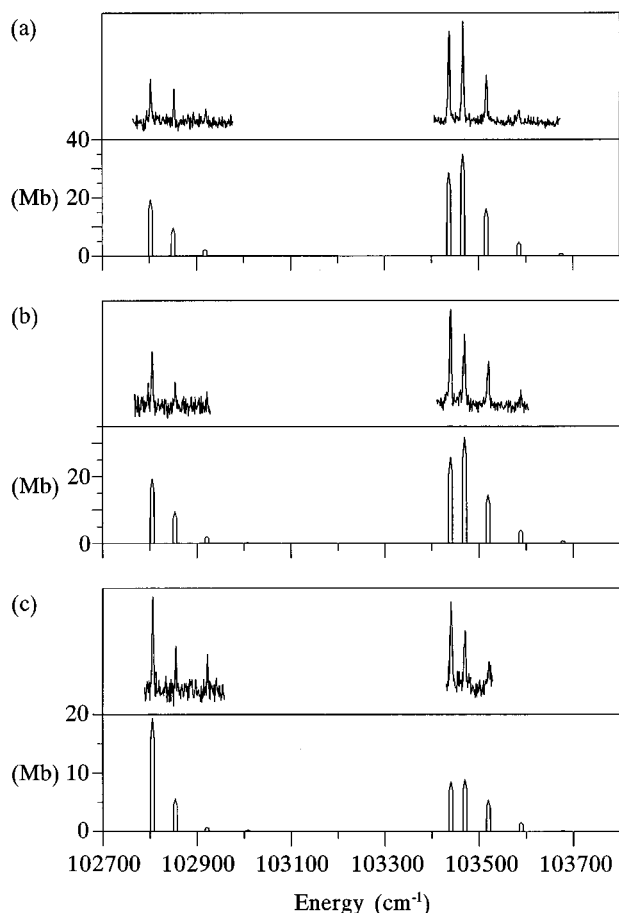


FIG. 6. ZEKE-PFI spectra resulting from ionization *via* the $S(0)$ rotational transition associated with the $F^1\Delta_2$ ($v'=0, J'=2e$) state of HCl. (a) Upper panel: observed with a static field of 5 V/cm pulsed to 10 V/cm after a time delay of 5 ± 5 ns. Lower panel: calculated for $n_{\text{field}}S = 160$, taking into account the population decay by spin-orbit and rotational autoionization after a delay of 5 ns. (b) Upper panel: observed with the same electric fields after a time delay of 30 ± 5 ns. Lower panel: calculated for $n_{\text{field}}S = 280$ after a delay of 30 ns. (c) Upper panel: observed with the same electric fields after a time delay of 105 ± 5 ns. Lower panel: calculated for $n_{\text{field}}S = 325$ after a delay of 105 ns.

perimental conditions. In fact, the comparison between Figs. 1 and 6(a) shows that variations in I_R of about 40% are observed for the short-time delay, leading to a factor 2 of difference between the calculated values of $D(n)$. Furthermore, it is observed in the experimental spectra that the results obtained *via* $P(3)$ are somewhat different from those obtained *via* the $S(0)$ transition. This difference has also been noted in Ref. 12 for the comparison between $R(1)$ and $S(0)$ transitions, and cannot be solely explained by alignment ef-

TABLE I. Dependence of dilution factor on time delay for ZEKE-PFI *via* the $S(0)$ transition to the $F^1\Delta_2$ state.

t (ns)	I_R (expt) ^a	I_R (calc)	$D(n)$
5	2.78	2.72	5.0
30	2.44	2.50	27.0
105	1.02	0.94	43.0

^aStatic field of 5 V/cm pulsed to 10 V/cm corresponding to $n_{\text{field}}=93$.

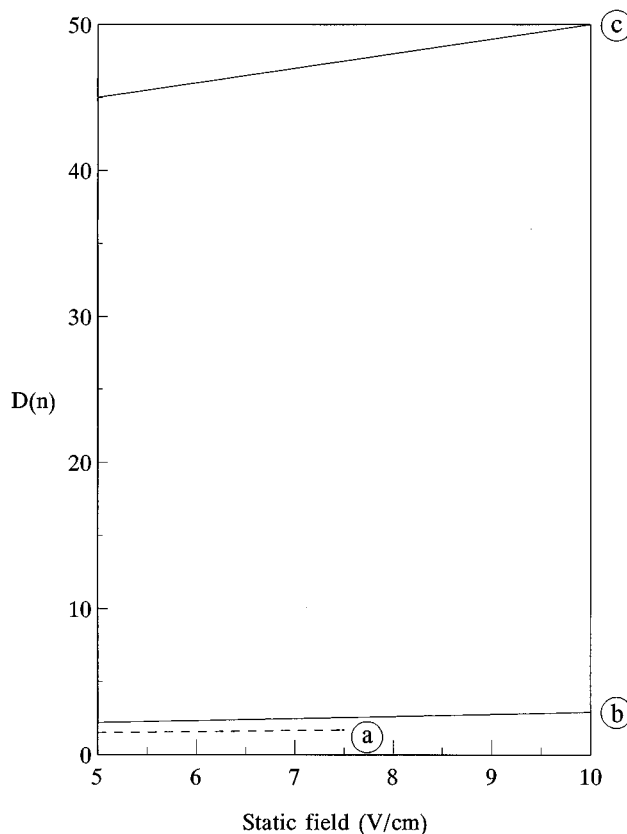


FIG. 7. Variation of $D(n)$ as a function of the static field and delay time. (a) Time delay 5 ns; bias+pulse field 12.5 V/cm; $P(3)$. (b) Time delay 5 ns; bias+pulse field 15.0 V/cm; $S(0)$. (c) Time delay 105 ns; bias+pulse field 15.0 V/cm; $S(0)$.

fects or different decay rates for e and f levels. Also, some details are not reproduced well by the calculations, in which it is assumed that the lengthening of the lifetime, induced by l mixing due to the static electric field, is the same for all rotational levels.¹³

Despite these inadequacies, the main conclusion persists: there is a stabilization of the branching ratio between the intensities of the two spin-orbit components upon an increase of the delay time. The same conclusion is obtained when the dependence on the bias field is considered for a constant total electric field: upon increasing the bias field the dilution factor becomes larger (see Fig. 7). In contrast, $D(n)$ is observed to remain about the same if the pulsed field is increased, but the bias field is kept constant. A theoretical study of the lifetime lengthening of high- n Rydberg states ($n \approx 100$) under the influence of the static electric field present during the time delay similar to the treatment of NO^{10} would be very useful in this particular case.

IV. CONCLUSIONS

The dependence of ZEKE-PFI spectra of HCl obtained after excitation of the $F^1\Delta_2$, $D^1\Pi_1$, and $f^3\Delta_2$ Rydberg states on the time delay, bias field, and pulsed electric field has been shown to give direct evidence for the dominating role of autoionization processes of high- n Rydberg states

during the waiting period in these experiments. The theoretical analysis of the spectra *via* the $F^1\Delta_2$ state demonstrates explicitly that the decay dynamics of the high- n Rydberg states are nonexponential, in agreement with previous theoretical conclusions based upon the influence of l mixing due to the Stark effect.

ACKNOWLEDGMENTS

The group at the University of Amsterdam gratefully acknowledges the Netherlands Organization for Scientific Research (N.W.O) for equipment grants and for financial support. Calculations performed by H.L.B. have used the French National Computer (CNUSC). One of the authors (H.L.B.) thanks James Martin for useful suggestions.

- ¹K. Müller-Dethlefs and E. W. Schlag, *Annu. Rev. Phys. Chem.* **42**, 109 (1991).
- ²R. G. Tonkyn, R. T. Wiedmann, and M. G. White, *J. Chem. Phys.* **96**, 3696 (1992).
- ³R. T. Wiedmann, M. G. White, H. Lefebvre-Brion, and C. Cossart-Magos, *J. Chem. Phys.* **103**, 10417 (1995).
- ⁴H. Lefebvre-Brion, *Chem. Phys. Lett.* **253**, 43 (1996).
- ⁵E. de Beer, B. G. Koenders, M. P. Koopmans, and C. A. de Lange, *J. Chem. Soc. Faraday Trans.* **86**, 2038 (1990).
- ⁶E. de Beer, W. J. Buma, and C. A. de Lange, *J. Chem. Phys.* **99**, 3252 (1993).
- ⁷N. P. L. Wales, W. J. Buma, and C. A. de Lange (unpublished results).
- ⁸F. Merkt, S. R. Mackenzie, and T. P. Softley, *J. Chem. Phys.* **103**, 4509 (1995).
- ⁹M. Bixon and J. Jortner, *J. Chem. Phys.* **103**, 4431 (1995).
- ¹⁰M. Bixon and J. Jortner, *J. Chem. Phys.* **105**, 1363 (1996).
- ¹¹N. P. L. Wales, W. J. Buma, C. A. de Lange, H. Lefebvre-Brion, Kwanghsi Wang, and V. McKoy, *J. Chem. Phys.* **104**, 4911 (1996).
- ¹²Y.-F. Zhu, E. R. Grant, Kwanghsi Wang, V. McKoy, and H. Lefebvre-Brion, *J. Chem. Phys.* **100**, 8633 (1994).
- ¹³W. A. Chupka, *J. Chem. Phys.* **98**, 4520 (1993).